Aβ and tau form soluble complexes that may promote self aggregation of both into the insoluble forms observed in Alzheimer's disease

Jian-Ping Guo*, Tetsuaki Arai†, Judit Miklossy*, and Patrick L. McGeer*‡

*Kinsmen Laboratory of Neurological Research, University of British Columbia, Vancouver, BC, Canada V6T 1Z3; and †Tokyo Institute of Psychiatry, 2-1-8 Kamikitazawa, Setagaya-ku, Tokyo 156-8585, Japan

To date, there is no reasonable explanation as to why plaques and tangles simultaneously accumulate in Alzheimer's disease (AD). We demonstrate here by Western blotting and ELISA that a stable complex can form between tau and amyloid-β protein (Aβ). This complex enhances tau phosphorylation by GSK3β, but the phosphorylation then promotes dissociation of the complex. We have localized the sites of this interaction by using peptide membrane arrays. Aβ binds to multiple tau peptides, especially those in exons 7 and 9. This binding is sharply reduced or abolished by phosphorylation of specific serine and threonine residues. Conversely, tau binds to multiple Aβ peptides in the mid to C-terminal regions of Aβ. This binding is also significantly decreased by GSK3β phosphorylation of tau. We used surface plasmon resonance to determine the binding affinity of Aβ for tau and found it to be in the low nanomolar range and almost 1,000-fold higher than tau for itself. In soluble extracts from AD and control brain tissue, we detected Aβ bound to tau in ELISAs. We also found by double immunostaining of AD brain tissue that phosphorylated tau and Aβ form separate insoluble complexes within the same neurons and their processes. We hypothesize that in AD, an initial step in the pathogenesis may be the intracellular binding of soluble Aβ to soluble nonphosphorylated tau, thus promoting tau phosphorylation and Aβ nucleation. Blocking the sites where Aβ initially binds to tau might arrest the simultaneous formation of plaques and tangles in AD.

immunochemistry | neurofibrillary tangles | senile plaques | surface plasmon resonance

So far, no reasonable interpretation has been advanced to explain the simultaneous appearance of senile plaques and neurofibrillary tangles (NFTs) in Alzheimer's disease (AD). Senile plaques develop extracellularly with the main component being aggregated amyloid-β protein (Aβ), whereas NFTs develop intracellularly with the main component being aggregated forms of phosphorylated tau. The two aggregation processes appear to occur independently, because NFTs develop in neuronal cell bodies and senile plaques develop around their nerve endings. This observation has led to two schools of thought regarding AD causation. The tau hypothesis holds that the disease is driven by tangles resulting from an excess of tau phosphorylation or a deficiency of its dephosphorylation (1). The hypothesis does not explain plaques. The amyloid hypothesis holds that the disease is driven by excess production of Aβ (2, 3). This hypothesis does not explain NFTs. Nevertheless, the amyloid cascade hypothesis is dominant because mutations in amyloid precursor protein (APP), which enhance Aβ production, cause autosomal dominant AD but not other types of dementia (2). On the other hand, mutations in tau that promote tau aggregation produce autosomal dominant frontotemporal dementia but not AD (4, 5). As a result, the presumption is that excess Aβ is a major cause and an upstream event of AD tangle formation, but exactly how an Aβ excess could induce subsequent tau aggregation is unclear.

Here we present evidence that Aβ binds strongly to tau in solution and hypothesize that this may be a precursor event to later self-aggregation of both molecules. The binding can be demonstrated by Western blotting, ELISA, and surface plasmon resonance. The binding enhances the phosphorylation of tau by GSK3β and acts as a site for Aβ nucleation into aggregates. The sites of mutual interaction have been identified on membrane arrays of overlapping tau and Aβ peptides including phosphorylation sites on tau that reduce the binding affinity.

We also present evidence, using soluble extracts of AD and control brain, that Aβ binds to tau in *in vivo* situations. We further show, using double immunofluorescence, that insoluble Aβ and tangled tau can be detected in the same neurons, indicating that both molecules have aggregated intracellularly at an early stage of the disease. This may represent an intermediate nucleation phase between the binding in solution of Aβ to nonphosphorylated tau and the eventual massive self-aggregation of both molecules. It suggests that prevention of AD might be achieved by blocking Aβ binding to tau.

Results

Western Blotting. To observe the formation of binding complexes between tau and Aβ *in vitro*, recombinant full length tau (T40) was mixed with Aβ40 or Aβ42 and incubated at 37°C for 5 h in a solution containing 40 mM Hepes (pH 7.5), 2 mM EGTA, and protease inhibitor mixture. Then, to examine the effect of this complex on tau phosphorylation, as well as the effect of tau phosphorylation on the strength of this complex, further incubations were carried out where the tau phosphorylating agent GSK3β was added to one set of duplicate tubes and all were incubated for a further 5 h at 30°C.

Samples were separated by SDS/10% PAGE under reducing conditions. Proteins in the gel were electrotransferred onto a poly(vinylidene difluoride) (PVDF) membrane. After blocking with 5% skim milk and 0.1% Tween 20 in TBS, membranes were incubated with a primary antibody for 1 h. After incubation with an appropriate horseradish peroxidase-conjugated secondary antibody, immunoreactivity was visualized by the chemiluminescence method using the ECL reagent, and recorded on Hyperfilm ECL. Blotted antibody was stripped from the membrane at 60°C for 2 h in 2% SDS, 100 mM 2-mercaptoethanol, and 62.5 mM Tris·HCl (pH 6.8) so that the membrane could be reprobed with another antibody.

The Western blot results are shown in Fig. 1. In Fig. 1*A*, it was initially probed with the antibody Tau 12 (1:50,000), which detects both phosphorylated and nonphosphorylated forms of tau. In Fig. 1*B*, the same blot was reprobed with the antibody 4G8 (1:200),
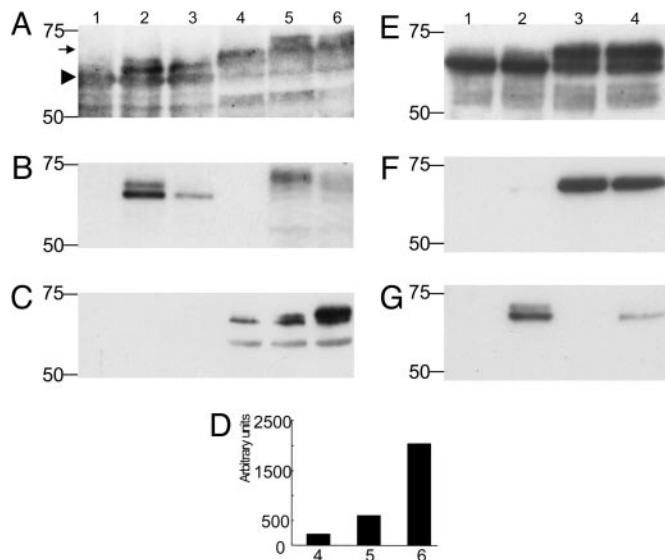
NEUROSCIENCE

Fig. 1. Western blotting of tau–Aβ complexes. (*A–C*) Western blotting after incubation of T40 only (lane 1), T40 plus Aβ40 (lane 2), T40 plus Aβ42 (lane 3), T40 plus GSK-3β (lane 4), T40 plus Aβ40 with GSK-3β (lane 5), and T40 plus Aβ42 with GSK-3β (lane 6) probed with antibodies Tau 12 (*A*), 4G8 (*B*), or PHF-1 (*C*). In *A* and *B*, the 30 μg/ml T40, 75 μg/ml Aβ40 and Aβ42, and 300 μg/ml GSK3β were used. The solutions were diluted 1:5 with SDS sample buffer, and 20 μl was loaded in each lane. In *C* and *D*, 5 μg/ml T40, 2.7 μg/ml Aβ40 and Aβ42, and 62.5 μg/ml GSK3β were used. The solutions were diluted 1:5 with SDS sample buffer, and 20 μl was loaded in each lane. In the samples of lanes 5 and 6, GSK-3β was added after incubation of T40 with Aβ40 and Aβ42. (*D*) Densitometric analysis of the bands in *C*. Each experiment was replicated twice with similar results. *E–G* illustrate the negative effect of tau phosphorylation on the formation of tau–Aβ binding. Phosphorylation of T40 by GSK-3β (300 μg/ml) preceded coincubation of T40 (25 μg/ml) and Aβ40 (62.5 μg/ml). Blots were probed with A0024 (*E*), PHF-1 (*F*), and tAβ40 (*G*). Lane 1, T40; lane 2, T40 plus Aβ40; lane 3, GSK-3β-treated T40; lane 4, GSK-3β-treated T40 plus Aβ40. Samples were diluted 1:5 with SDS sample buffer, and 20 μl was loaded in each lane. Molecular weight markers are shown on the left. See *Results* for interpretation of the bands.

which detects both Aβ40 and Aβ42. In Fig. 1*C*, a similar blot was probed with PHF-1 (1:200), a phosphorylation-dependent anti-tau antibody.

In Fig. 1*A*, a band of 64 kDa corresponding to nonphosphorylated T40 can be seen in all lanes (arrowhead). The band is very weak in lanes 4, 5, and 6, indicating that most of the T40 was phosphorylated. Additional bands at ≈67 and 70 kDa are seen in lane 2, which correspond to T40 complexes with monomers and dimers of Aβ40. Only one weak additional band is seen in lane 3 that corresponds to T40 complexing with Aβ42. Lanes 4, 5, and 6 show a prominent new band at 71 kDa corresponding to phosphorylated T40 (arrow). Lane 5 shows a further band at ≈74 kDa corresponding to a complex of Aβ40 with phosphorylated T40. However, note that this band is much weaker than the corresponding band in lane 2 of the nonphosphorylated T40–Aβ40 complex.

In Fig. 1*B*, where the membrane was reprobed with 4G8, no bands were observed in lanes 1 and 4 because no Aβ was present. A doublet at 67 and 70 kDa was observed in lane 2 corresponding to monomer and dimer Aβ40 complexes with T40. In lane 3, only a monomer complex was observed with Aβ42. In lane 5, a weak band was observed at ≈74 kDa, indicating some residual binding of Aβ40 to phosphorylated T40. The band in lane 5 was weaker than in lane 2. No band was observed in lane 6, indicating that no detectable complex could be observed between phosphorylated T40 and Aβ42. These results establish that SDS stable complexes may form between tau and Aβ40 and Aβ42, but that phosphorylation of tau reduces the degree of binding.

In Fig. 1*C*, there were no immunoreactive bands in lanes 1–3,

which had only nonphosphorylated tau. Bands with increasing intensity were observed with GSK-3β-treated T40 without Aβ (lane 4), with Aβ40 (lane 5), and with Aβ42 (lane 6). The immunoreactive bands on the films were digitized with a CanoScan D660U scanner. The relative quantities were determined by densitometric analysis using NIH IMAGE version 1.62 (Fig. 1*D*). These results indicate that Aβ peptides enhance phosphorylation of tau by GSK-3β and that Aβ42 is a much more powerful enhancer than Aβ40.

Then, to examine the effect of tau phosphorylation on the strength of binding of Aβ to tau, the order was reversed so that T40 was phosphorylated before the addition of Aβ. T40 and GSK3β were incubated for 5 h at 30°C as described (6). Then, Aβ40 was added and incubation carried out for another 5 h at 37°C. The reactions were stopped by the addition of SDS sample buffer and boiling. For controls, T40 alone, T40 plus Aβ40 without GSK-3β, or T40 plus GSK-3β without Aβ40 were treated in the same way.

Fig. 1 *E–G* shows the results of the first probe with A0024 (1: 30,000), a phosphorylation-independent polyclonal antibody to tau (Fig. 1*E*); reprobing with PHF-1, a phosphorylation-dependent antibody (Fig. 1*F*); and reprobing with tAβ40, which recognizes the terminal sequence of Aβ40 (Fig. 1*G*). With A0024 probing (Fig. 1*E*), a 64-kDa tau band was observed in all lanes, but was weaker in lanes 3 and 4 because of tau phosphorylation. In the samples of GSK3β-treated T40 only (lane 3) and GSK3β-treated T40 plus Aβ40 (lane 4), an intense 71-kDa band appeared, indicative of this phosphorylation. In the sample of unmodified T40 plus Aβ40 (lane 2), an additional weak band of 67 kDa was observed, demonstrating the presence of a tau–Aβ complex. In Fig. 1*F*, PHF-1 stained a 71-kDa band in lanes 3 and 4, but failed to stain lanes 1 and 2 because of the absence of phosphorylated tau. Upon probing with tAβ40 (Fig. 1*G*), a significant doublet of 67 and 70 kDa appeared in lane 2, but only a weak band of 67 kDa was observed in lane 4. These results establish that prior phosphorylation of tau inhibits the formation of a tau–Aβ complex.

Detection of Tau–Aβ Interaction Sites on Membrane-Bound Peptide Arrays. The general methods for preparing multiple overlapping peptides bound to cellulose membranes have been described in detail (7). For Aβ peptide membranes, the robotic synthesizer was programmed to prepare 24 overlapping decamers covering the sequences in Aβ starting at the β-secretase cut site with each decamer shifted by 2 aa through the γ-secretase cut site. The initial peptide was KMDAEFRHDS, and the final peptide was IVITLVMLKK. The array covered two lines of 12 spots each (Fig. 2*A*).

For tau, 15-mer peptides were synthesized based on the human full length tau sequence of 441 aa (NCBI protein ID AAC04279.1). A total of 214 peptide spots were prepared, commencing with MAEPRQEFEVMEDHA, with each subsequent spot shifted by 2 aa toward the C terminus ending with TLADEVSLAKQGL. The arrays were synthesized in 18 lines with 12 spots to each line, with the terminal line (L in Fig. 2*B*) having only 10 spots. Additionally, tau peptides were prepared so that each serine and threonine was substituted by phosphoserine and phosphothreonine.

The results are shown in Figs. 2 and 3, Table 1, and Table 2, which is published as supporting information on the PNAS web site. When the Aβ peptide membrane was probed with nonphosphorylated tau (T40), and detected with tau 2 antibody, there were cluster areas binding to tau (Fig. 2*A* and Table 1). These were in the middle and C-terminal Aβ regions. The core peptides in these clusters, i.e., the sequences common to adjacent peptides binding to tau, were EVHHQK (Aβ11-16), NKGAII (Aβ27-32), and GGVVIA (Aβ37-42). These core peptides are presumed to be the ones binding most strongly to tau.

When the Aβ peptide membrane was probed with phosphorylated T40 by GSK3β and detected with the phosphorylation-dependent antibody anti-tau [pT231], binding to the first two clusters
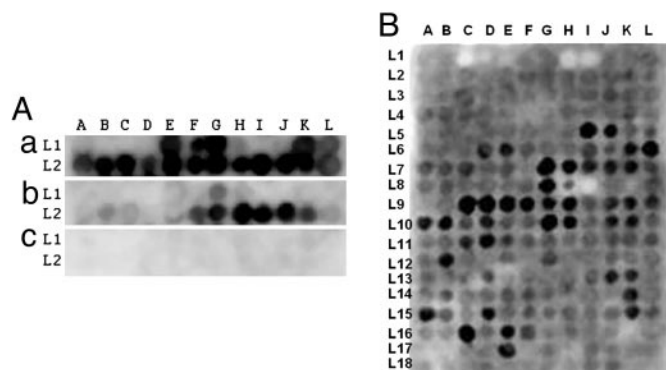
Fig. 2. Interaction of recombinant T40 and phosphorylated T40 on Aβ 10-mer peptide array membranes, and Aβ1-42 on Tau 15-mer peptide array membrane. (*A*) 10 μg/ml recombinant T40 (*a*) or phosphorylated T40 by GSK-3β (*b*), or vehicle solution only (*c*), in 50 mM ammonium acetate (pH 6.5), 3 μM heparin (MW 6000), and 0.1 mM PMSF solution probed on Aβ 10-mer peptide array membrane, developed with ECL reagent after incubating with tau-2 monoclonal antibody and HRP–anti-mouse IgG conjugate (*a* and *c*), tau phosphorylation-dependent antibody pT[231], and HRP–anti-rabbit IgG conjugate (*b*). (*B*) 10 μg/ml of Aβ1-42 in PBS probed on Tau 15-mer peptide array membrane, developed with ECL reagent after incubating with 4G8 monoclonal antibody and HRP–anti-mouse IgG conjugate.

was abolished and binding to the C-terminal cluster was significantly reduced (Fig. 2*A*). When the membrane was probed without the addition of tau, there was no signal, indicating no cross reaction with the antibodies used. These results demonstrate the areas where tau can bind to Aβ. They also illustrate that tau phosphorylation eliminates binding to all Aβ40 regions and reduces it to weak binding at the C terminus of Aβ42 only.

When the tau peptide membrane was probed with Aβ42 and detected with 4G8 antibody, there were 19 binding clusters, as illustrated in Fig. 2*B* and detailed in Table 2. When the membrane was probed with vehicle in place of Aβ, there was no signal, indicating that the 4G8 primary antibody and horseradish peroxidase-labeled secondary antibody did not cross react with tau peptides (data not shown). Strong signals spanning several contig-
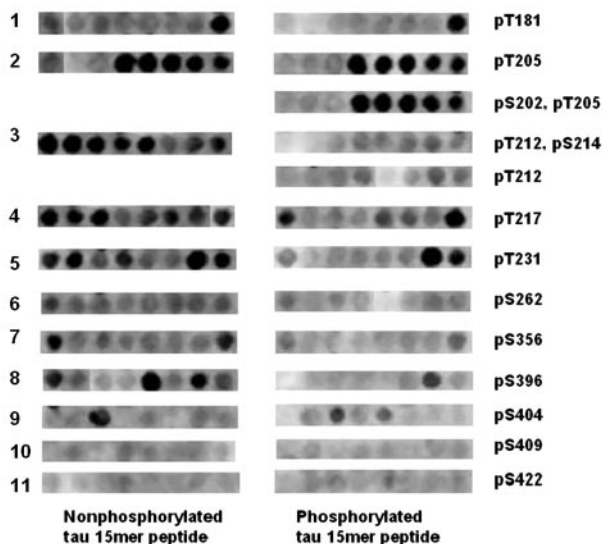
Fig. 3. Comparison of Aβ1-42 probing on 11 regions of tau where serine and threonine residues were either phosphorylated or not phosphorylated. The 15-mer peptide arrays were probed with Aβ1-42 (10 μg/ml in PBS). They were developed with ECL reagent after incubating with 4G8 monoclonal antibody and HRP–anti-mouse IgG conjugate.

uous spots were located on peptides from exons 7 and 9 of tau protein. There was no reaction signal on peptides from exons 1–3, and only single or weak signals from peptides from exons 10–12 (Fig. 3*B* and Table 2).

When the phosphorylated tau peptide membrane was probed with Aβ42, binding to a number of peptides was eliminated or reduced. These are shown in Fig. 3 and Table 3, which is published as supporting information on the PNAS web site. Phosphorylation of T212, S214, S356, and S396 completely blocked Aβ42 binding. Phosphorylation of T217 and T231 decreased the binding significantly. Phosphorylation of T181, S202, and T205 was without effect. These results illustrate that Aβ can bind to multiple peptides in tau, especially in exons 7 and 9, and that this binding is reduced or eliminated by phosphorylation of certain tau peptides.

Surface Plasmon Resonance. Surface plasmon resonance is a technique for quantitating protein–protein interaction (8, 9). Experiments were performed by using a Biacore 3000 instrument, and results were analyzed with the BIAEVALUTION 4.1 software (Biacore International AB, Uppsala, Sweden). The results are shown in Fig. 5, which is published as supporting information on the PNAS web site. The association constants (K_A, $1/M$) of tau protein (T40) binding to immobilized T40, Aβ42 and Aβ40 are 2.15×10^4, 1.55×10^7, and 2.05×10^7, respectively. The dissociation constants (K_D, M) are 4.65×10^{-5}, 6.45×10^{-8}, and 4.87×10^{-8}, respectively. These experiments demonstrate that the affinity of tau for Aβ42 and Aβ40 are in the nanomolar range and nearly 1,000-fold higher than T40 for itself.

ELISAs. Initially, to determine the range where linear responses were obtained, test ELISA experiments were performed with A0024 as the capture antibody and 4G8 as the detection antibody. A0024 recognizes the C-terminal segment of tau, and 4G8 recognizes the Aβ17-24 sequence, so they do not overlap with the regions where Aβ binds to tau as demonstrated on membrane arrays. Recombinant tau (T40) at 10 μg/ml or 40 μg/ml was incubated with serial concentrations of Aβ42. A linear range of 4–64 μg of Aβ was found (data not shown). Accordingly, standard solutions containing 10 μg of tau and 32 and 64 μg of Aβ42 were incubated to compare results using different capture and detection antibodies. When the antibodies were reversed so that the tau–Aβ complex was captured with the monoclonal Aβ antibody 4G8, and tau detected with the polyclonal antibody A0024, a dose dependency was also observed. With Aβ58-68, a different polyclonal tau antibody that recognizes the N-terminal region and is phosphorylation independent, a dose dependency with 4G8 was again observed. When the tau capture antibody was switched to the monoclonal HT7, which is phosphorylation independent and also recognizes an N-terminal sequence, and the Aβ detection antibody switched to the polyclonal R17, a dose dependency was once more observed. These data establish that tau–Aβ complexes form in solution which can be captured with either an Aβ or tau antibody and detected with the counterpart antibody. Detailed results are shown in Table 4, which is published as supporting information on the PNAS web site.

Using the A0024 capture and 4G8 detection assay, we examined soluble fractions from five AD and five control brains for soluble tau–Aβ complexes. Signals were detected in all 10 samples, providing putative evidence of such complexes in human brains. The average signals from AD brains were modestly higher than from control brains ($P = 0.074$). The soluble brain extracts contain many proteins and various protein complexes so the interpretation of these data requires considerable caution and further exploration is required. Detailed results are published as Table 5, which is published as supporting information on the PNAS web site.

Results of Immunohistochemistry. Immunohistochemical results by confocal microscopy are shown in Fig. 4 and Movie 1, which is published as supporting information on the PNAS web site. Fig. 4

Table 1. Interaction of recombinant T40 and phosphorylated T40 to Aβ 10-mer peptide array membrane

Spot	Sequence (N- to C-terminal)	Position in Aβ	Reaction to Aβ array membrane	
			r-T40	p-T40
1EFG	α	11-16	+	-
	DSGY**EVHHQK**			
	GY**EVHHQK** LV			
	EVHHQK↓LVFF			
1K	FFAEDVGSNK	19-27	+	-
2ABCDE	DVGS**NKGAII**	26-36	+	-
	GS**NKGAIIGL**			
	NKGAIIGLMV			
	GAIIGLMVGG			
	IIGLMVGGVV			
2FGHIJK	γ₁ γ₂	37-46	+	+
	GLMV**GGVV** IA			
	MVGGVV IA TV			
	GGVV IA TVIV			
	VV IA TVIVIT			
	IA↓TVIVITLV			

The cutting sites of secretases are indicated. α, α-secretase cutting site; γ₁, γ-secretase cutting site of Aβ1-40; γ₂, γ-secretase cutting site of Aβ1-42; r-T40, recombinant T40; p-T40, phosphorylated T40. The core region is shown in bold letters.

A–C illustrates colocalization of Aβ, as detected by 4G8 (red fluorescent secondary antibody), and tau, as detected by A0024 (green fluorescent secondary antibody), within a viable neuron in the hippocampus of an AD case. Fig. 4*D* is a merged photomicrograph at lower power showing a few neurons with varying degrees of colocalization of tau and Aβ (yellow fluorescence) along with others immunostaining for tau only (green immunofluorescence), indicating that colocalization is not universally observable. Nevertheless, this result establishes that Aβ cannot only be found intracellulary but that it can also be identified in an insoluble state. Fig. 6, which is published as supporting information on the PNAS web site, illustrates a comparable result using the polyclonal antibody tAβ42 to detect insoluble intracellular Aβ and the monoclonal antibody C3 to detect intraneuronal tau tangles.

Discussion

We have shown by Western blotting, ELISA, and surface plasmon resonance that there is a high affinity between Aβ and tau and that stable complexes form between the two in solution. The surface plasmon resonance affinity constants of tau for Aβ40 and Aβ42 are almost 1,000-fold higher than tau for itself. They are in the low nanomolar range comparable to the 20 nanomolar affinity previously reported by Hasegawa *et al.* (9) for Aβ40 to immobilized fibrillar Aβ.

We have also shown by Western blotting that both Aβ40 and Aβ42 when complexed with tau enhance its phosphorylation by GSK-3β, and that Aβ42 has a greater capacity to do so than Aβ40.

It has been reported that Aβ42 enhances tau phosphorylation by tau protein kinase II (10).

We have determined, using peptide membrane arrays, that the probable sites of tau–Aβ interaction are sequences in exons 7 and 9 of tau and the mid to C-terminal sequences of Aβ. Peptides of tau phosphorylated at T212, S214, S356, and S396 completely block Aβ binding and phosphorylation of T217, and peptides of tau phosphorylated at T231 decrease it significantly. Conversely, phosphorylation of recombinant tau by GSK3β abolishes interaction with all Aβ40 sequences and substantially weakens it for the terminal Aβ42 sequence.

We have shown by ELISA that there is a concentration-dependent binding of Aβ to tau in solutions containing both molecules. We have also shown that signals indicative of tau–Aβ complexes can be detected by ELISA in soluble extracts of control and AD brain tissue.

In AD brain, we have confirmed the existence of Aβ deposits in the same intracellular structures as tau deposits by confocal immunohistochemistry. Although such colocalization is small compared with the extracellular deposits of Aβ, it may represent the footprint of a much larger interaction occurring in the soluble state.

These data are not predicted by the standard model of APP localization (11). The standard model depicts APP as a cell surface receptor with a single transmembrane region, a large extracellular N-terminal domain, and a short intracellular C-terminal domain. Because γ-secretase, the final cleaving enzyme that produces Aβ, is intramembranous, Aβ is presumed to be produced at the cell surface and then secreted.
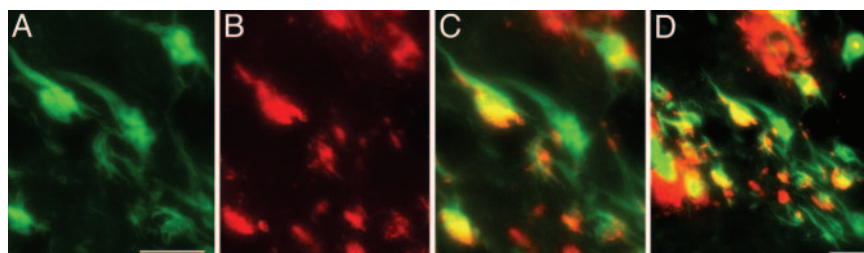
Fig. 4. Coexpression of Aβ and tau in neurofibrillary tangles. (*A–C*) Tau (A0024 labeled with Hilyte Fluor 488) exhibiting a green fluorescence (*A*) and Aβ (4G8 labeled with Hilyte Fluor 555) showing red fluorescence (*B*) are coexpressed in tangle bearing neurons of the entorhinal cortex in a case of AD as shown by the yellow fluorescence in the merged image (*C*). (*D*) A lower-power merged image showing a mixture of tangled neurons coexpressing Aβ and tau (yellow color) and tau only (green color) as well as extracellular Aβ deposits (red color). (Scale bars, 50 μm *A* and 100 μm in *D*.)

Guo *et al.*

This standard model, originally proposed in 1987, predicts that APP is localized to the surface of neurons in both normal and AD brain (11). Such a localization has never been reported. Instead, antibodies to diverse sequences in APP immunostain punctuate granules within the cytoplasm of normal appearing neurons in both control and AD cases. These are concentrated in the perinuclear region and extend into neuronal processes (12–16). The nature of these granules is unknown, but they indicate that APP accumulates intracellularly.

Some APP must be metabolized to Aβ intracellularly because intracellular Aβ precipitates have also been reported to be present not only in AD (17–20) but in Down syndrome cases as well (21). Gyure et al. (21) found that, in Down syndrome cases, intraneuronal precedes extraneuronal Aβ deposition. Deposition of such insoluble deposits must be preceded by soluble Aβ accumulation. Gouras et al. (20) consider that intraneuronal Aβ42 accumulation is an early pathological step in AD neuropathology. They have recovered Aβ40 and Aβ42 from lysates of NT2 neuroblastoma cells that were concentrated in fractions enriched in Golgi and endoplasmic reticulum (18). Others have found in cultured cells intracellular Aβ accumulation derived from the Golgi network and endoplasmic reticulum (18, 22–26). Piccini et al. (27), using immunoprecipitation, have identified Aβ species in soluble extracts of frozen AD and control brain (27, 28), but did not examine for tau complexes. Lue et al. (29) detected, by ELISA, Aβ40 and Aβ42 in soluble extracts of frozen entorhinal and superior frontal cortex from AD cases, high pathology controls, and normal controls with AD cases showing the highest level of both Aβ species.

The eventual fate of the accumulated intracellular Aβ is unknown. D'Andrea et al. (17) conclude that lysis of neurons which have accumulated intracellular Aβ deposits accounts for much of the extracellular amyloid material. Laferla et al. (30) have identified intracellular Aβ in granular cytoplasmic structures and also conclude that death of neurons results in extracellular deposition of this material. Grundke-Iqbal et al. (31) have identified granular Aβ deposits in the same neurons as thioflavin S-positive NFTs in AD hippocampus.

Taken together, these data indicate that there is a significant intraneuronal pool of soluble Aβ in both control and AD cases that is probably generated in the Golgi apparatus and in the endoplasmic reticulum. This soluble Aβ would be available to interact with soluble tau to promote tau phosphorylation and act as nucleation site for insoluble Aβ accumulation. Insoluble Aβ is detectable in the same neurons as NFTs and may eventually be extruded because of its lower molecular weight, whereas phosphorylated tau, aggregating as insoluble filaments, may become trapped due to its higher molecular weight. Eventually, neurons with NTFs die, leaving ghost tangles along with any accumulated intraneuronal Aβ deposits. Such a mechanism would not exclude the direct secretion of Aβ from the outer membrane of a neuron into the extracellular space with subsequent nucleation into extracellular amyloid deposits. However, it does suggest that it is the intracellular pool that promotes the formation of tangles.

Giasson et al. (32) have shown that coincubation of tau and α-synuclein promotes fibrillation of both proteins (32), so there is precedent for the mechanism suggested here. Our data may also help to explain the results of Gotz et al. (33), who found that injection of Aβ fibrils into the brains of P301L mutant tau transgenic mice caused 5-fold increases in the numbers of cell body NFTs. Most importantly, our data suggest that interference with the binding of Aβ and tau might be the earliest and most effective step for preventing AD.

Materials and Methods

Reagents. Recombinant human tau 40 (2N4R, T40), a kind gift of M. Goedert (Cambridge University, Cambridge, U.K.), was expressed in E. coli BL21(DE3) and purified as described (6). Aβ1-40

and Aβ1-42 were bought from AnaSpec (San Jose, CA). GSK-3β was purchased from EMD Biosciences (San Diego, CA).T46 anti-tau monoclonal antibody was bought from Zymed. Rabbit polyclonal anti-tau A0024 was purchased from DAKO. Goat polyclonal anti-tau AB 5868 was purchased from Chemicon, and HT7 anti-tau monoclonal was purchased from Innogenetics (Gent, Belgium). Tau 12 and tau C3 were generous gifts from L. I. Binder (Northwestern University, Chicago). All are independent of tau phosphorylation. PHF-1, an anti-phosphorylated tau monoclonal antibody was a kind gift from Peter Davies (Albert Einstein College of Medicine, New York). Anti-tau [pT231] was purchased from BioSource (Camarillo, CA). The 4G8 monoclonal antibody to Aβ, which recognizes Aβ17-24, and therefore detects Aβ40, Aβ42, and N-terminal truncated forms of Aβ, was obtained from Sigma. The polyclonal antibodies tAβ40, which recognizes the C terminus of Aβ40, and tAβ42, which recognizes the C terminus of Aβ42, were generous gifts of H. Mori (Tokyo Institute of Psychiatry, Tokyo). R17, a rabbit polyclonal antibody that recognizes Aβ1-23, was a generous gift of T. Ishii (Tokyo Institute of Psychiatry, Tokyo).

Tissues. Five cases of AD (average age, 75.4 years; range, 69–78 years) and five without neurological disease (average age, 76 years; range, 63–93 years) were selected from our Kinsmen Laboratory brain bank for ELISA analysis. The AD cases all met National Institute of Neurological and Communication Disorders and Stroke/Alzheimer's Disease and Related Disorders Association criteria for definite AD. Frozen brain tissue from frontal or temporal cortex was homogenized with a Teflon-glass homogenizer in 5 volumes of Tris-buffered saline (TBS, 50 mM Tris·HCl, pH 7.6/150 mM NaCl) with added protease inhibitor mixture (Roche Diagnostics). After centrifugation at $100,000 \times g$ for 1 h, the supernatant fraction was taken.

Brains from an additional five AD cases (average age, 78.2 years; range, 63–87 years) and one control (age 59) were selected for immunohistochemical analysis. Again, definite AD was confirmed by neuropathological examination of all five AD cases.

Immunofluorescent Staining and Confocal Microscopy. Samples (30 μm thick) were cut on a freezing microtome from paraformaldehyde-fixed blocks and processed for immunohistochemistry in the free-floating state. The sections were treated with 100% formic acid (151162; MO Biomedicals, Eschwege, Germany) for 20 min. After three 5 min washes in PBST, they were incubated in 5% BSA solution at room temperature for 40 min. The sections were incubated overnight at room temperature with a monoclonal antibody recognizing Aβ17-24 (4G8) and a polyclonal antibody recognizing tau (A0024), diluted in PBST containing 2% BSA and 1% normal goat serum. After washing in PBST, Hilyte Fluor 488-labeled goat anti-rabbit IgG (H+L) was applied in PBST containing 10% normal goat serum for 1 h, giving a green fluorescence. After washing the sections (three times for 5 min) in PBST, incubation with Hilyte Fluor 555-labeled goat anti-mouse IgG (H+L) was similarly carried out giving a red fluorescence. To visualize cell nuclei, after washing the sections in PBST, Hoechst dye 3258 (1 μg/ml) staining was performed for 10 min. Sudan black staining (10 min) was used to quench autofluorescence. After a rinse in PBS, the sections were mounted with Fluoromont G (Southern Biotechnology, Birmingham, AL). The sections were examined by confocal microscopy. Staining cell nuclei by Hoechst dye produced a white fluorescence in UV light, which was changed to a blue color in the merged fluorescent images.

Microtiter Plate Binding Assay. The plates were coated at 4°C overnight with one of four different capture antibodies diluted in sodium carbonate buffer (pH 9.6). The antibodies were A0024 (30 μg/ml, anti-tau polyclonal); AB 5868 goat serum (1:200, anti-tau N-terminal polyclonal); HT7 (5 μg/ml, anti-tau N-terminal monoclonal); and 4G8 (5 μg/ml, Aβ monoclonal). The microwells were

blocked with 5% BSA in TBS 0.2% Tween 20 (TBS-T0.2) buffer at 37°C for 2 h and washed five times with TBS-T0.2 buffer. A total of 100 μl of samples were pipetted into duplicate wells and incubated at 37°C for 1 h. The microwells were then treated with the appropriate detection antibody.

With A0024 and AB 5868 as the tau capture antibodies, bound Aβ was detected by incubating the wells at 37°C for 1 h with 2 μg/ml of the anti-Aβ monoclonal antibody 4G8. The microwells were washed with buffer and incubated at 37°C for 1 h with 1:20,000 rabbit anti-mouse IgG–HRP conjugate. The wells were developed with TMB solution at room temperature for 15 min. The reaction was stopped with 10% H_2SO_4, and the optical density was measured at 450 nm by using a Multiskan spectrophotometer. With the anti-tau monoclonal antibody HT7 as the capture antibody, bound Aβ was detected with the anti-Aβ rabbit serum R17 (1:20,000) followed by treatment with anti-rabbit–HRP (Sigma) and detected as before. With the anti-Aβ monoclonal antibody as the capture antibody, bound tau was detected with A0024 (6 μg/ml) followed by treatment with anti-rabbit–HRP and detection as before. For controls, similarly treated solutions containing tau alone or Aβ alone were added to the wells.

For detection of tau–Aβ complexes in tissue, 100 μl of supernatant was added directly to wells coated with A0024 and detection with 4G8 carried out as before.

Preparation of Peptide Arrays Bound to Cellulose Membranes and Probing with Aβ and Tau. The general methods for preparing multiple overlapping peptides bound to cellulose membranes have been described in detail (7). Reagents included Amino-PEG cellulose membranes and Fmoc-amino acids obtained from Intavis (San Marcos, CA). N,N'-diisopropylcarbodiimide, 1-hydroxybenzotriazole, trifluoroacetic acid, piperidine, triisobutylsilane, and dichloromethane were purchased from Sigma, and N-α-Fmoc-O-benzyl-L-phosphoserine and N-α-Fmoc-O-benzyl-L-phosphothreonine were purchased from AnaSpec (San Jose, CA).

The Aβ peptide membranes were probed with 10 μg/ml purified recombinant T40 or T40 phosphorylated by GSK3β. Incubation was carried out in a solution of 50 mM ammonium acetate (pH 6.5), 3 μM heparin (MW 6000), and 0.1 mM PMSF at 37°C overnight. After this treatment, 10 μg/ml tau-2 antibody in 1% skim milk or 1:500 diluted pT^{231} polyclonal antibodies were used for probing.

The tau peptide membranes were probed with 10 μg/ml freshly prepared Aβ42 peptide in 10 mM PBS overnight at 37°C. After washing with 10 mM Tris·HCl, pH 7.4/150 mM NaCl/0.2% Tween 20 (TBS-T0.2), the membranes were blocked with 5% skim milk in TBS-T0.2 at 37°C for 2 h and then incubated with 10 μg/ml 4G8 antibody in 1% skim milk at 37°C for 2 h.

The membranes were washed with TBS-T0.2 and then treated at 37°C with 1:4,000 HRP-labeled rabbit anti-mouse IgG for 1 h. After a final wash, the membranes were visualized by using Bio-Rad Fluorescent Imager after developing with ECL Western blotting detection reagent (Amersham Pharmacia). Control membranes were probed with PBS only.

Surface Plasmon Resonance. Three different channels of a carboxylated dextran CM5 chip (Biacore) were immobilized with recombinant T40 protein, Aβ42, and Aβ40 peptides, respectively, as the test channels, with one channel as the blank control by using the amine coupling protocol of the manufacturer. All binding experiments were performed by using HBS-EP buffer (0.01 M Hepes, pH 7.4/0.15 M NaCl/3 mM EDTA/0.005% surfactant P20) as a baseline control or diluent of recombinant T40 protein at 25°C at a flow rate of 2 μl/min; 40, 80, 320, 640, and 1280 nM concentrations of recombinant T40 protein, Aβ42, and Aβ40 were prepared freshly with HBS-EP buffer.

1. Iqbal, K., Alonso Adel, C., Chen, S., Cholan, M. O., El-Akkad, E., Gong, C. X., Khatoon, S., Li, B., Liu, F., Rahman, A., *et al.* (2005) *Biochim. Biophys. Acta* **1739,** 198–210.
2. Hardy, J. A. & Higgins, G. A. (1992) *Science* **256,** 184–185.
3. Hardy, J. & Selkoe, D. J. (2002) *Science* **297,** 353–356.
4. Hutton, M. (2002) *Movement Disorders* **17,** 1402–1403.
5. Goedert, M. & Jakes, R. (2005) *Biochim. Biophys. Acta* **1739,** 240–250.
6. Arai, T., Guo, J. P. & McGeer, P. L. (2005) *J. Biol. Chem.* **280,** 5145–5153.
7. Guo, J. P., Petric, M., Campbell, W. & McGeer, P. L. (2004) *Virology* **324,** 251–256.
8. Jonsson, U., Fagerstam, L., Ivarsson, B., Johnsson, B., Karlsson, R., Lundh, K., Lofas, S., Persson, B., Roos, H., Ronnberg, I., *et al.* (1991) *BioTechniques* **11,** 620–627.
9. Hasegawa, K., Ono, K., Yamada, M. & Naiki, H. (2002) *Biochemistry* **41,** 13489–13498.
10. Rank, K. B., Pauley, A. M., Bhattacharya, K., Wang, Z., Evans, D. B., Fleck, T. J., Johnston, J. A. & Sharma, S. K. (2002) *FEBS Lett.* **514,** 263–268.
11. Kang, J., Lemaire, H. G., Unterbeck, A., Salbaum, J. M., Masters, C. L., Grzeschik, K. H., Multhaup, G., Beyreuther, K. & Muller-Hill, B. (1987) *Nature* **325,** 733–736.
12. McGeer, P. L., Akiyama, H., Kawamata, T., Yamada, T., Walker, D. G. & Ishii, T. (1992) *J. Neurosci. Res.* **31,** 428–442.
13. Benowitz, L. I., Rodriguez, W., Paskevich, P., Mufson, E. J., Schenk, D. & Neve, R. L. (1989) *Exp. Neurol.* **106,** 237–250.
14. Cole, G. M., Masliah, E., Shelton, E. R., Chan, H. W., Terry, R. D. & Saitoh, T. (1991) *Neurobiol. Aging* **12,** 85–91.
15. Card, J. P., Meade, R. P. & Davis, L. G. (1988) *Neuron* **1,** 835–846.
16. Shivers, B. D., Hilbich, C., Multhaup, G., Salbaum, M., Beyreuther, K. & Seeburg, P. H. (1988) *EMBO J.* **7,** 1365–1370.
17. D'Andrea, M. R., Nagele, R. G., Wang, H. Y., Peterson, P. A. & Lee, D. H. (2001) *Histopathology* **38,** 120–134.
18. Greenfield, J. P., Tsai, J., Gouras, G. K., Hai, B., Thinakaran, G., Checler, F., Sisodia, S. S., Greengard, P. & Xu, H. (1999) *Proc. Natl. Acad. Sci. USA* **96,** 742–747.
19. Takahashi, R. H., Milner, T. A., Li, F., Nam, E. E., Edgar, M. A., Yamaguchi, H., Beal, M. F., Xu, H., Greengard, P. & Gouras, G. K. (2002) *Am. J. Pathol.* **161,** 1869–1879.
20. Gouras, G. K., Tsai, J., Naslund, J., Vincent, B., Edgar, M., Checler, F., Greenfield, J. P., Haroutunian, V., Buxbaum, J. D., Xu, H., *et al.* (2000) *Am. J. Pathol.* **156,** 15–20.
21. Gyure, K. A., Durham, R., Stewart, W. F., Smialek, J. E. & Troncoso, J. C. (2001) *Arch. Pathol. Lab. Med.* **125,** 489–492.
22. Xu, H., Sweeney, D., Wang, R., Thinakaran, G., Lo, A. C., Sisodia, S. S., Greengard, P. & Gandy, S. (1997) *Proc. Natl. Acad. Sci. USA* **94,** 3748–3752.
23. Skovronsky, D. M., Doms, R. W. & Lee, V. M. (1998) *J. Cell Biol.* **141,** 1031–1039.
24. Cook, D. G., Forman, M. S., Sung, J. C., Leight, S., Kolson, D. L., Iwatsubo, T., Lee, V. M. & Doms, R. W. (1997) *Nat. Med.* **3,** 1021–1023.
25. Wild-Bode, C., Yamazaki, T., Capell, A., Leimer, U., Steiner, H., Ihara, Y. & Haass, C. (1997) *J. Biol. Chem.* **272,** 16085–16088.
26. Hartmann, T., Bieger, S. C., Bruhl, B., Tienari, P. J., Ida, N., Allsop, D., Roberts, G. W., Masters, C. L., Dotti, C. G., Unsicker, K., *et al.* (1997) *Nat. Med.* **3,** 1016–1020.
27. Piccini, A., Russo, C., Gliozzi, A., Relini, A., Vitali, A., Borghi, R., Giliberto, L., Armirotti, A., D'Arrigo, C., Bachi, A., *et al.* (2005) *J. Biol. Chem.* **280,** 34186–34192.
28. Tabaton, M. & Piccini, A. (2005) *Int. J. Exp. Pathol.* **86,** 139–145.
29. Lue, F., Kuo, Y., Roher, A. E., Brachova L., Shen, Y., Sue, L., Beach, T., Kurth, J. H., Rydel, R. E. & Rogers, J. (1999) *Am. J. Pathol.* **155,** 853–862.
30. LaFerla, F. M., Troncoso, J. C., Strickland, D. K., Kawas, C. H. & Jay, G. (1997) *J. Clin. Invest.* **100,** 310–320.
31. Grundke-Iqbal, I., Iqbal, K., George, L., Tung, Y. C., Kim, K. S. & Wisniewski, H. M. (1989) *Proc. Natl. Acad. Sci. USA.* **86,** 2853–2857.
32. Giasson, B. I., Forman, M. S., Higuchi, M., Golbe, L. I., Graves, C. L., Kotzbauer, P. T., Trojanowski, J. Q. & Lee, V. M. (2003) *Science* **300,** 636–640.
33. Gotz, J., Chen, F., vanDorpe, J. & Nitsch, R. M. (2001) *Science* **293,** 1446–1447.